ORIGINAL PAPER-PRODUCTION ENGINEERING

Effect of acid treatment on the geomechanical properties of rocks: an experimental investigation in Ahdeb oil field

Usama Alameedy[1] · Ayad A. Alhaleem[1] · Abubakar Isah[2] · Ahmed Al-Yaseri[3] · Mohamed Mahmoud[2] ·
Ibrahim Saeb Salih[4]

Abstract

Acidizing is one of the most used stimulation techniques in the petroleum industry. Several reports have been issued on the difficulties encountered during the stimulation operation of the Ahdeb oil field, particularly in the development of the Mishrif reservoir, including the following: (1) high injection pressures make it difficult to inject acid into the reservoir formation, and (2) only a few acid jobs have been effective in Ahdeb oil wells, while the bulk of the others has been unsuccessful. The significant failure rate of oil well stimulation in this deposit necessitates more investigations. Thus, we carried out this experimental study to systematically investigate the influence of acid treatment on the geomechanical properties of Mi4 formation of the Mishrif reservoir. The acid core-flood experiments were performed on seven core samples from the oil reservoir in central Iraq. The porosity, permeability, acoustic velocities, rock strength, and dynamic elastic parameters were computed before and after the acidizing treatment. To determine the optimal acid injection rate, different injection flow rates were used in the core-flooding experiments. The propagation of an acid-induced wormhole and its effect on the rock properties were analyzed and compared to that of intact rocks. Computed tomography (CT) scan and a 3D reconstruction technique were also conducted to establish the size and geometry of the generated wormhole. To analyze the influence of mineralogical variation and heterogeneity and confirm the consistency of the outcomes, acidizing experiments on different rock samples were conducted. The results demonstrate that for all the rock samples studied, the mechanical properties exhibit rock weakening post-acid treatment. The Young's modulus reduced by 26% to 37%, while the Poisson's ratio, the coefficient of lateral earth pressure at rest, and the material index increased by 13% to 20%, 23% to 32%, and 28% to 125%, respectively. The CT scan visually confirmed that the acid treatment effectively creates a pathway for fluid flow through the core.

Keywords Acidizing · Wormhole · Rock mechanical properties · Rock petrophysical properties · Core flooding

List of symbols

E	Young's modulus (Pa)
PR	Poisson's ratio
IM	Material index
K_o	Lateral earth pressure at rest coefficient
V_p	Longitudinal (compressional) wave velocity (m s^{-1})
V_s	Transverse (shear) wave velocity (m s^{-1})
P	Longitudinal (compressional) wave (m)
S	Transverse (shear) waves (m)
ρ	Density (kg m^{-3})
W_{dry}	Weight of the dry plugs (kg)
W_{sat}	Weight of the saturated cores (kg)
W_{brine}	Weight of the brine saturating the rocks (kg)
V_{pore}	Pore volume (m^3)
V_{bulb}	Bulk volume (m^3)
ϕ_e	Effective porosity
Q	Instantaneous flow rate (m^3 s^{-1})
K	Permeability (μm^2)
μ	Dynamic viscosity of brine (Pa s)
A	Cross-sectional area (m^2)

✉ Ahmed Al-Yaseri
  ahmed.yaseri@kfupm.edu.sa

1   Petroleum Engineering Department, University of Baghdad, Baghdad, Iraq

2   College of Petroleum Engineering and Geosciences, King Fahd University of Petroleum and Minerals, Dhahran 31261, Saudi Arabia

3   Center of Integrative Petroleum Research (CIPR), College of Petroleum Engineering and Geoscience, King Fahd University of Petroleum and Minerals, Dhahran 31261, Saudi Arabia

4   Lukoil Company, Basra, Iraq

l	Length of the core (m)
ΔP	Pressure drop (Pa)
T	Transit time (s)

Introduction

Acid treatment is an effective and efficient well-stimulation technique, and it has been applied extensively to stimulate carbonate reservoirs (Gomaa et al. 2018; Guo et al. 2014; Ituen et al. 2017; Zhu et al. 2015). In acid stimulation, fracture acidizing and matrix acidizing are two distinct subcategories. On one hand, matrix acidizing involves removing formation damage that impairs the permeability around the wellbore caused by drilling fluid invasion/fines migration; on the other hand, acid fracturing enhances the connectivity between the well and reservoir by creating pathways that penetrate deep into the reservoir referred to as wormholes (Al-Arji et al. 2021; Shafiq et al. 2018). In this regard, wormholing has been experimentally investigated and summarized by many authors (Al-Arji et al. 2021; Dong 2018; Xue et al. 2018). Al-Arji et al. (2021) and Xue et al. (2018) studied wormholing mechanisms where the rock minerals were dissolved by the contacting acid to form cylindrical pores during the wormholing process. Typically, acid fracturing yields better results in formations with low permeability and low confining stress or hard rocks. Conversely, acidizing is more effective in soft formations with high permeability and high confining stress (Schwalbert et al. 2020). Various acid treatment techniques, such as acid jetting and CO_2 energized acid treatment, have been presented to improve acidizing effectiveness (Beckham et al. 2015; Ndonhong et al. 2016).

Several researchers investigated the mechanism of acid-rock reactions, acidizing fluid efficiency, acid flowback mechanism, acid leakoff, and the acidizing models (Aljawad et al. 2020; Ghommem et al. 2015; Li et al. 2015; Lungwitz et al. 2007; Yoo et al. 2018; Zhang et al. 2020a, b, c; Zhu et al. 2015). On the other hand, others investigated the effect of acid treatment on the mechanical rock structure (Zhang et al. 2020b) and the influence of the rock mineralogy on acidizing efficiency (Martyushev et al. 2022). Various acidizing fluids such as self-diverting acid (Bazin et al. 1999; Lungwitz et al. 2007), visco-elastic surfactant (VES) acid, gelled acid, self-generated acids, and recently, emulsified acid (Martyushev and Vinogradov 2021) and chelating agents (Tariq et al. 2021) have been developed and investigated both in the laboratory and in field-scale (Gou et al. 2021; Hassan and Al-Hashim 2017; Isah et al. 2021a, b; Kiani et al. 2021; Lai et al. 2021; Li and Shi 2021; Martyushev and Vinogradov 2021; Melendez et al. 2007; Taylor and Nasr-El-Din 2001).

In the acid treatment of naturally fractured carbonate formation, VES acid forms more complex fractures compared

to self-generated acid and gelled acid. However, gelled acid is capable of decreasing the rock's breakdown pressure significantly (up to 57% less than that achievable by water fracturing), thus increasing fracture propagation and enhancing efficiency (Gou et al. 2021). Moreover, gelled acid creates larger wormholes compared to crosslinked acid; consequently, it weakens the rock's mechanical properties more than crosslinked acid (Lai et al. 2021). Stimulation success depends on the length and width of these wormholes (Al-Arji et al. 2021); thus, a successful acid treatment operation requires that the wormhole propagates deep into the formation.

In radial acid treatment experiments of hollow chalk samples, Walle and Papamichos (2015) demonstrated that acidizing rock samples causes a reduction in the rock's mechanical strength, and this was confirmed by comparing the mechanical properties of the acid-treated rocks and the intact ones. Mustafa et al. (2022) studied the impact of acid wormholes on the mechanical properties of carbonates (chalk, limestone, and dolomite), and their findings indicate that acidizing reduces the hardness and elastic modulus of the rocks. The authors noted that dolomite was the least impacted by the acid treatment, while chalk samples were affected the most. Barri et al. (2016) investigated the effect of acidizing using chelating agents (ethylenediaminetetraacetic acid [EDTA] and diethylenetriaminepentaacetic acid [DTPA]) on the mechanical properties of carbonate rocks. The outcome showed that the elastic properties of weak carbonates (such as Austin chalk) were most affected, while hard rocks such as Indiana limestones were not significantly affected. Zhou et al. (2021) experimentally researched fracture surface strength before and after acid treatment. The authors argued that several reported mechanical deteriorations of carbonate rocks after acid etching could not be applied to evaluate fracture conductivity since such investigations provide information on the mechanical properties of the rock mass rather than the surface of the fracture. They emphasized that fracture surface strength measurement data before and after acid etching is necessary for fracture optimization and conductivity evaluation of the acidizing job. The work of Li and Shi (2021) also showed that acid fracturing can alter rock strength.

Certainly, the acid dissolution of rock minerals modifies the rock structure, the mineralogy, as well as the mechanical properties of the artificial fracture surface (Liu and Mostaghimi 2017). Therefore, acidizing often leads to modifications in the rock's mechanical properties around the wormhole; consequently, it improves or impairs reservoir quality. A notable body of literature reported rock weakening due to acidizing as reservoir impairment; however, rock loosening may imply the generation of flow paths by the acid dissolution of the rock and the consequent wormhole propagation into the reservoir. Several reports have been issued on

the difficulties encountered during the stimulation operation of the Ahdeb oil field, particularly in the development of the Mishrif reservoir, including the following: (1) high injection pressures make it difficult to inject acid into the reservoir formation; and (2) only a few acid jobs have been effective in Ahdeb oil wells, while the bulk of the others has been unsuccessful. This called for more investigations. Thus, we carried out this experimental study to systematically investigate the influence of acid treatment on the geomechanical properties of Mi4 formation of the Mishrif reservoir in Iraq. The propagation of an acid-induced wormhole and its effect on the rock strength were analyzed and compared to that of intact rocks. CT scan was also conducted to establish the size and shape of the fractures generated. The findings of this investigation provide a better understanding of the acid treatment of carbonates; thus, comprehensive planning and implementation of acidizing jobs in the Mishrif reservoir can be accomplished.

Materials and methods

Geological and petrophysical properties of Mishrif reservoir

The thin section photomicrographs of the cored sections of Mishrif reservoir's well ADM12 used for this study are shown in Fig. 1. A total of seven (7) rock samples were used in this investigation: samples 1–4 were extracted from section A (composed mainly of echinoderm, green algae, and micrite limestone), while samples 5–7 were cored from section B (micrite, orbitolina sand grains, and limestone). Both sets (sections A and B) were composed mainly of calcite mineral and 1–1.5% clay content, and the filling material was micrite. Table 1 shows the mineral composition of the experimental core samples obtained using X-ray diffraction (XRD) analysis. There are 34 zones interpreted in this well, and an aggregate of 135.8 m is accumulated with the overall thickness of the 19 oil and oil-poor zones. The entire thickness is 57.2 m, with seven transition zones. There are 8 water zones with an overall thickness of 150.8 m. A comprehensive description of the geological and fluid properties of this reservoir is provided in the appendices.

The wireline logging data of Mishrif reservoir's well ADM12 for petrophysical evaluation is provided in Fig. 2. It is necessary to distinguish between oil-rich and oil-poor zones. The oil-rich zones exhibit higher resistivity, the oil saturation of these zones is higher than 47 percent, and its effective porosity is greater than 15 percent. The shale volume of most oil zones is typically less than 10 percent. Overall, the Mishrif

Table 1 Mineral composition of target formation and experimental core samples obtained using XRD

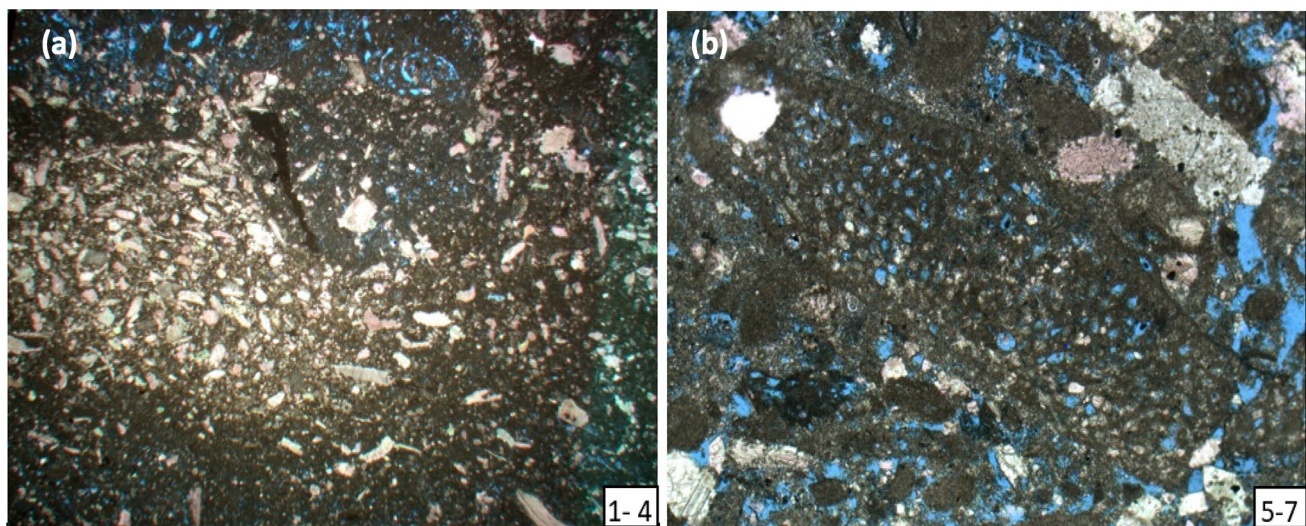| Samples no	Calcite (%)	Clay (%)	Fluorite (%)	Pyrite (%)
1–4	98	1.0	0.5	0.5
5–7	98	1.5	0	0.5

Fig. 1 Photomicrographs for the two cored sections of the Mishrif reservoir's well ADM12. **a** corresponds to samples 1–4 from section A: The texture is characterized by biological burrows, the internal ring is composed of echinoderm, and the core is composed of gastropods and green algae. The overall texture consists of echinoderm, green algae, micrite, large globigerina, and beehive worms. **b** corresponds to samples 5–7 from section B: The limestone is predominated by orbitolina debris by strong solution, also named orbitolina sand grains. Visible dividual orbitolina and echinoderm with a large number of sand grains with a strong solution and dense gathering can be observed

Fig. 2 Wireline logging interpretation for well ADM12
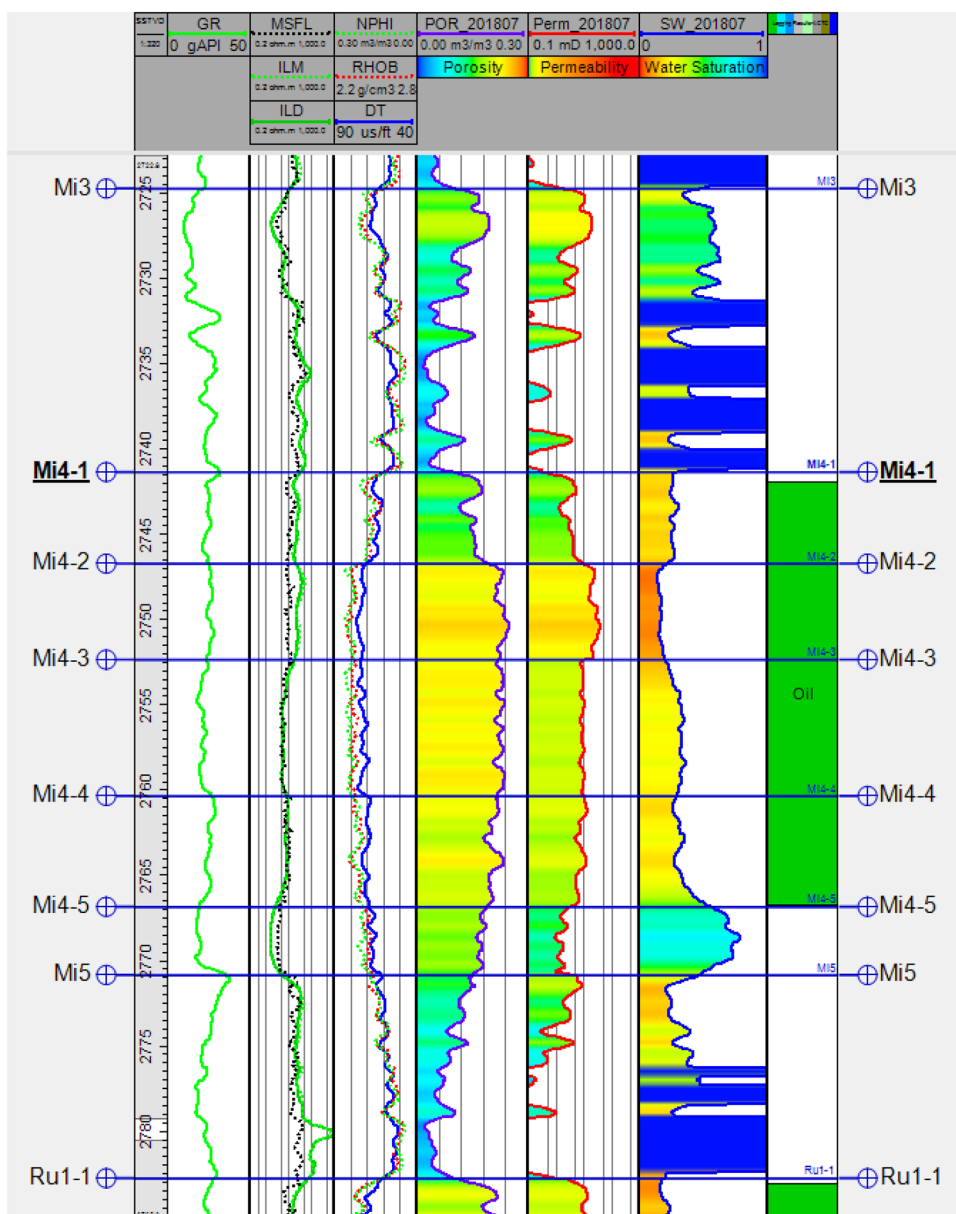
zone is an oil layer with an effective porosity of around 22 percent and an oil saturation of about 84 percent. Before chemical treatment, we determined the porosity and permeability of seven rock samples from the Mi4 unit in the Mishrif formation. According to core and well logs analysis for all Mishrif units, permeability values range from 0.1 to 57 mD. However, the permeability ranges 0.17–15.2 mD have been measured for the seven examined plugs. The petrophysical parameters of the Mishrif reservoir are summarized in Table 2.

Samples preparation

After coring, seven core samples were cut into the required dimensions (2.526 cm in diameter and a length of 4.571 cm each). To prepare the samples for strength tests and coreflooding experiments, the ends of the cores were ground to a smooth and parallel surface using end-face grinding. Solvents (toluene and alcohol) were used to clean the core plugs and prepare them for the measurements. Toluene was used to clean

Table 2 Mishrif reservoir's petrophysical parameters

Well	Formation	Interval(MD) (m)	Thickness (m)	Net_Pay (m)	Avg. PRO (%)	Avg.PERM (mD)	SW (%)
ADM12	Mi4	2740.1–2765.9	24.8	22.6	19.535	9.748	31.676

any residual oil in the rocks while alcohol was used to remove precipitated salt within the rock's pores (Al-Yaseri et al. 2022; Isah et al. 2021a, b).

Basic properties of gelled acid

Acid diversion is critical for stimulating vertical wells with extended target zones or horizontal wells in carbonates (Bazin et al. 1999). Increased viscosity of the injected acid and a delay in the acid interaction with the formation are two benefits of in situ gelled acids that improve treatment efficiency. Additionally, the gel should break down quickly as the acid is depleted, allowing for better clean-up when the acid treatment is completed (Taylor and Nasr-El-Din 2001). Table 3 shows the properties of the gelled acid. It is noteworthy that the viscosity of reacted acid is only 3 mPa s (around that of water); therefore, it can be concluded that there was no adverse effect such as formation damage by the acidizing fluid to the fracture and formation after the acidizing operation.

Core-flooding experiment

Core-flooding tests were conducted based on acid injection to establish wormholes in the plugs. Figure 3 shows a schematic of the core-flooding system. The core holder is connected downstream of the ISCO pump and the fluids (acid and brine) accumulator, and it is provided with pressure gauges to measure confining pressure and pressure drop across the core plug. The data acquisition system was used to monitor and collect data on the core-flooding process. The optimal injection rate was determined after seven acidizing experiments using varying flow rates. The flow rate ranged from 0.667 to 6.67 cc/min. The core samples were vacuumed with a vacuum pump to ensure full saturation and then saturated with brine (see Table 4 for brine specifications) for 2 h; afterward, the samples were left in the desiccator for 48 h. An ENERPAC pump was used to provide a confining pressure of 2000 psi to the core plugs for all core-flooding experiments. To maintain a constant flow with minimal pressure variations, brine was injected first through the ISCO pump. The inlet and outlet pressures at various injection rates were recorded to determine the liquid permeability of the core samples using Darcy's law. Acid was then injected until the wormhole was created as indicated by a sharp pressure drop. Pressure and injection volumes were monitored and controlled using the core-flooding system's monitoring and control unit.

Porosity and permeability measurements

Pre- and post-acidizing core plug porosity and permeability measurements were performed. The gravimetric or saturation technique for calculating porosity was employed. Pore volume is calculated (Eq. 2), and porosity was then computed using Eq. 3:

$$W_{brine} = W_{sat} - W_{dry} \tag{1}$$

$$V_{pore} = W_{brine}/\rho_{brine} \tag{2}$$

$$\phi_e = V_{pore}/V_{bulk}. \tag{3}$$

W_{dry} is the weight of the dry plugs, W_{sat} is the weight of the saturated cores, and W_{brine} is the weight of the brine saturating the rock's pores. Permeability was assessed using flowing fluids with known viscosity through a core sample with known dimensions and then measuring the flow rate and pressure drop. In this work, we utilized brine flow through the plug and employed the Darcy law (Eq. 4) to compute liquid permeability:

$$Q = -\frac{KA}{\mu}\frac{\Delta P}{l}, \tag{4}$$

where Q is the instantaneous flow rate (m³ s⁻¹), K is the permeability (μm²), μ is the dynamic viscosity of brine (Pa s), ΔP is the pressure drop across the rock plug (Pa), and A

Table 3 Basic properties of gelled acid

Items	Test result
Appearance	Red-brown viscous uniform liquid
Viscosity, 170 s⁻¹, 25 ℃, mPa s	25
Viscosity, 170 s⁻¹, 90 ℃, 60 min, mPa s	20
Static corrosion rate, 90 ℃, g/m² h	4.79
Surface tension, mN/m	23.75
The capability of stabilizing ferric ion, mg/mL	> 100
The viscosity of reacted acid, mPa s	3
The chemical concentration of the gelled acid	15% HCl
Gelling agent (polyacrylamide)	2.5 wt %
Corrosion inhibitor	1.5% ADT-1 and 6% ADZ-1

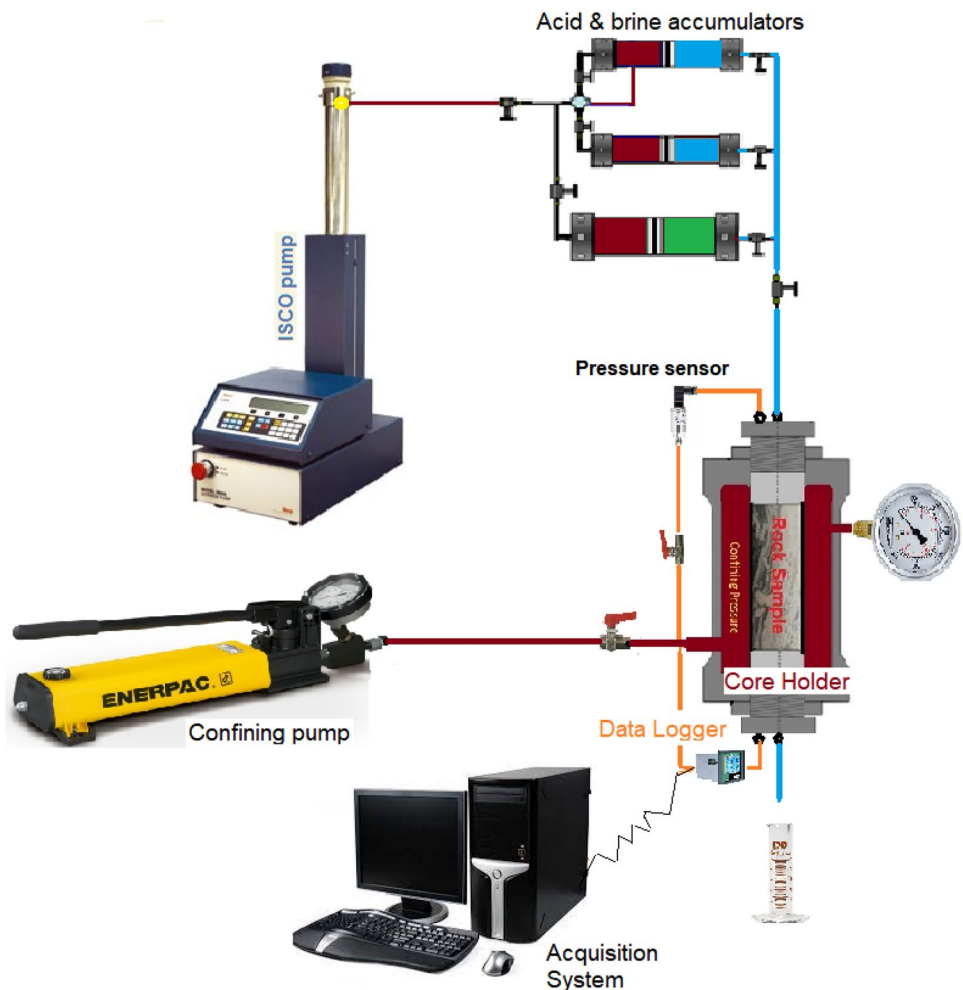**Fig. 3** Schematic diagram of the core-flooding system

Table 4 Brine composition in ppm

Test	pH	Sp. Gr	TDS	Organic Matter	Ca^{2+}	Mg^{2+}	Na^+	HCO_3^-	SO_4^-	Cl^-
Results	7.2	1.0068	15,100	(–)	620	484	4231	246	3267	6252

(m^2) and l (m) are the cross-sectional area and length of the core, respectively.

Determination of rock geomechanical properties

Surface rock hardness, acoustic velocities, and dynamic elastic parameters were determined before and after the acidizing treatment. To analyze the elastic and geotechnical features of the carbonate rocks in this study, longitudinal (V_p) and transverse (V_s) wave velocities were measured for all samples before and after acidizing. The measurements were performed using the Sonic viewer (Model-5217A). A core plug connects the two transducers, one of which acts as a transmitter and the other as a receiver. Ultrasonic transducers are installed on both parallel sides to measure the core's transit time (T), which is determined by delivering a series of ultrasonic impulses through the core sample. Sample length (L) is divided by the transit time (T) of the propagated waves to obtain the velocity of the compressional and shear waves (V_p and V_s). All core samples were analyzed for significant geotechnical characteristics based on the values of the velocities (V_p and V_s). The combination of these findings was utilized to evaluate the subsurface rock's properties. Analysis of elastic and petrophysical characteristics before and after acid injection was carried out using the mechanical properties of the rock.

Young's modulus (E) is one of the most important geomechanical properties of rocks. It is a measure of the rock's stiffness, that is, the material's resistance against being compressed (or extended) due to applied stress. The Young's modulus of the rock samples is computed using Eq. 5 before and after acid treatment using the

compressional and shear waves velocities (V_p and V_s) (Fjær et al. 2008). Poisson's ratio (PR) indicates the ratio of the lateral expansion (or contraction) deformation to long-term extension deformation. For the majority of mineral deposits, the Poisson's ratio is in the range of 0 to 0.5, with more rigid, competent, and incompressible rocks having a lower Poisson's ratio and vice versa (Abd El-Rahman et al. 1992; Domenico 1984), and it is computed using Eq. 6.

$$E = \frac{\rho V_s^2 \left(3V_p^2 - 4V_s^2\right)}{V_p^2 - V_s^2} \tag{5}$$

$$PR = \frac{0.5(V_p/V_s)^2 - 1}{(V_p/V_s)^2 - 1}. \tag{6}$$

The elasticity of materials is impacted by several factors including the content of the material, the degree of consolidation, joints, fractures, and the presence of fluids in porous structures, all of which influence the material index (Shirani et al. 2010). The lateral earth pressure at rest coefficient (K_o) shows the degree of the strength and consolidation of rocks. It is in the range of 0 to 1 for most materials. As with Poisson's ratio, this coefficient decreases with densely consolidated sediments and rises with loose, unconsolidated sediments (Al-Awsi and Khorshid 2021). The material index (IM) and lateral earth pressure at rest coefficient (K_o) were computed using Eqs. 7 and 8, respectively.

$$IM = \frac{3 - (V_p/V_s)^2}{(V_p/V_s)^2 - 1} \tag{7}$$

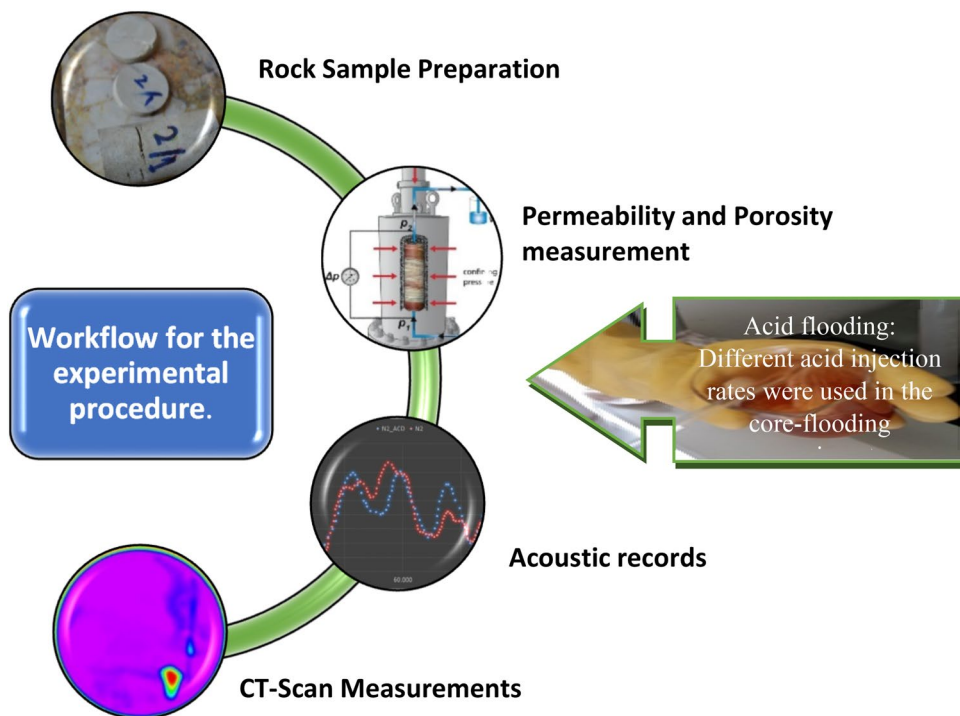$$K_O = \frac{(V_p/V_s) - 2}{(V_p/V_s)^2}. \tag{8}$$

Computed tomographic (CT) scanning

CT scanning was used to examine the size and geometry of the wormholes in each rock sample. Helical acquisition 140 kV and 500 mAs resolution CT images were taken to see the micro-scale alterations generated by the chemical interaction between acid solution and the core materials. The mechanical characteristics of various rock types are affected by the size of the wormholes created. The overall workflow for the experimental approach is shown in Fig. 4.

Results and discussion

The porosity, permeability, acoustic velocities, rock strength, and dynamic elastic parameters were computed before and after the acidizing treatment to establish the reasons behind the difficulties encountered during the acid stimulation operation of the Ahdeb oil field, particularly in the development of the Mishrif reservoir. Thus, we systematically analyzed the influence of acid treatment on the petrophysical and geomechanical properties of Mi4

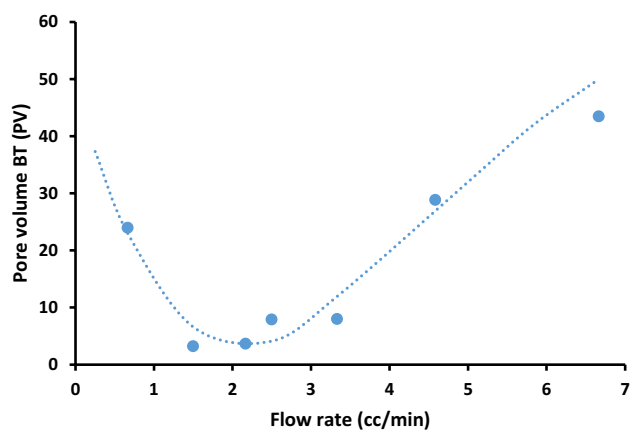**Fig. 4** Schematic diagram of the workflow for the experimental procedure

Fig. 5 Pore volume at breakthrough vs. injection rate for acidizing experiments

Fig. 6 The effect of PVBT on the improvement of porosity

Effect of acid treatment on geomechanical properties

The geomechanical properties including the acoustic parameters (V_s and V_p) of the rock samples were determined after acidizing treatment. The following subsections provide a comparative analysis of the pre- and post-acid-treated rocks.

Impact of acid treatment on acoustic properties

Various factors affect the seismic velocities of rocks, among which are density, lithology, mineralogy, porosity, grain size, stress levels, joints and fractures, pore fluid, anisotropy, and temperature. These parameters (i.e., the seismic velocities) are used to compute the rock geomechanical properties such as the elasticity modulus or Young's modulus (E), Poisson's ratio (PR), and rock material index (IM) of rocks (Dobrin 1976).

The compressional (P) and shear (S) waves of all plugs were monitored before and after the acid experiment to confirm the alteration of the ultrasonic waves due to acid treatment. A comparison between the ultrasonic waveforms of acid-treated samples of rocks and those of intact saturated samples of rock was performed. Ultrasonic waveforms for both intact and treated cores are shown in Fig. 7, illustrating how wormholes and fluid flow alter velocity, amplitude, and frequency for plug sample No.1. The acid-treated sample's P-wave arrival time is longer compared to that of the intact rock, and the S-wave amplitude is more significant compared to the intact rock's relatively low amplitudes. P-wave signals from untreated and treated rock have somewhat differing frequencies.

Impact of porosity and wormhole on the elastic characteristics of rock

An inverse correlation between effective porosity and compressional velocity (V_p) was established in this work, as

formation of the Mishrif reservoir. Acid efficiency curves were constructed using core-flooding tests on core samples (see Fig. 5). Ultimately, the goal is to discover the injection rate that results in the least quantity of acid being used throughout the process (Safari et al. 2014). Typically, the best injection rate results in the most optimal wormhole, reducing the amount of acid pore volume injection. In this regard, the reaction rate and convective mass transfer are the factors that regulate the wormholing process. Due to face dissolution, substantial amounts of acid are consumed before the wormhole can break through at low injection rates. Consequently, conical-shaped wormholes are formed. However, when the injection rate is substantially greater than the reaction rate, branching wormholes are formed. This was corroborated in the work of Mustafa et al. (2022).

Thus, the development of a wormhole is maximized at a certain Damkohler number (i.e., the ratio of reaction rate to mass transfer). In this study, the rock samples yielded the lowest breakthrough injected pore volume of 3.7 PV at 2.16 cc/min; thus, this was considered the optimum injection rate. However, at 0.67 cc/min and 6.67 cc/min, the pore volume at breakthrough (PVBT) measured around 24 and 43.5 PV, respectively. The effects of PVBT on the elastic characteristics of the rock samples are detailed and analyzed in the subsequent section. The acidizing treatment resulted in a considerable increase in porosity for each of the rock samples. A positive relationship between PVBT and the relative increase in porosity for all rock plugs was observed as can be seen in Fig. 6. The greater the PVBT was, the more likely the relative porosity increased. This finding can be attributed to increased rock dissolution/etching as more PV is injected.
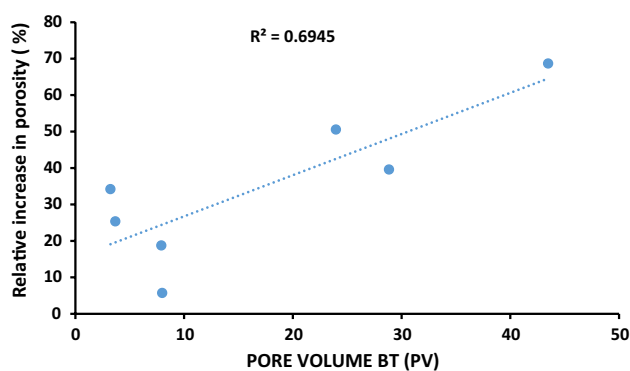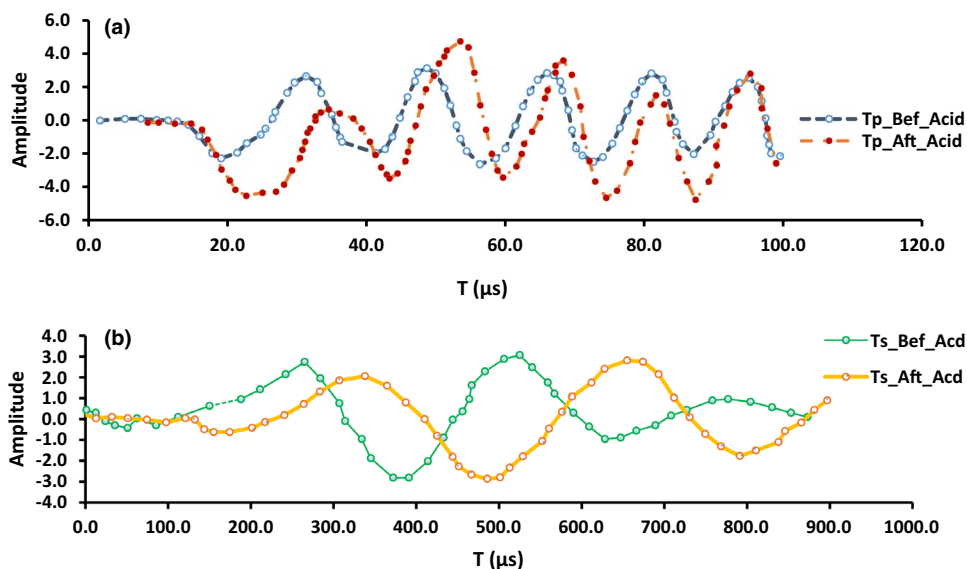
Fig. 7 Representative waveforms recorded in plug sample No.1 for **a** the P-wave (blue before acidizing and red after acidizing) and **b** the S-wave (green before acidizing and orange after acidizing) pulse

shown in Fig. 8. This finding is in line with the work of other researchers (Jermy and Bell 1998; Marques 1998). However, rocks with a high porosity before acid treatment but a persistent network of wormholes after acid treatment have a propagation velocity that is lower compared to that of rocks predominated by pores as compared to micropores. In general, the higher the porosity is, the lower the propagation velocity is. Figure 9 illustrates the relationship between porosity and shear wave. It is consistent with the trend in compressional velocity before acid treatment; however, the relationship between porosity and shear wave (V_s) is less obvious after acid treatment. This is due to the rock structural modification by acid dissolution. As the porosity increases, V_s demonstrates a lower decline as compared to the slope before acid flooding. Based on the established positive relationship between PVBT and the relative increase in porosity of the rock plugs, it can be concluded that an

increase in PVBT will likely result in an increase in porosity and a consequent decrease in the values of the acoustic properties of the rock.

Rock mechanical properties pre- and post-acid treatment

This section compares the findings of the dynamic elastic properties, that is, Young's modulus, Poisson's ratio, lateral earth pressure at rest coefficient, and material index obtained before and after acidizing. Formations can be damaged by drilling and production activities, and factors such as the migration of fines and mud invasions may alter the permeability around the wellbore (Shafiq et al. 2018). Completion activities may cause a change in pressure and flow rate in a wellbore, and this is known as a mechanical skin factor (Furui et al. 2008; Yildiz 2006). Damage around the wellbore formation might lead to further pressure drops in the

Fig. 8 Relationships between the velocity of compressional waves (V_p) and effective porosity before and after acid treatment
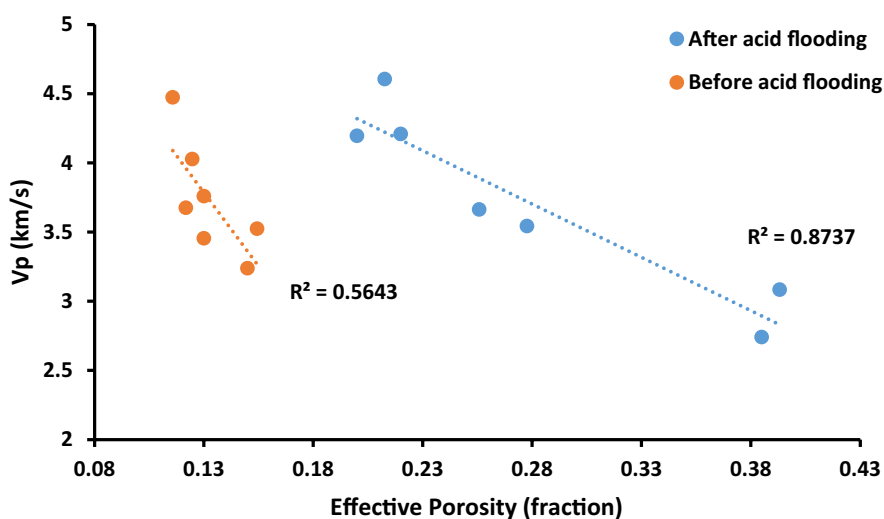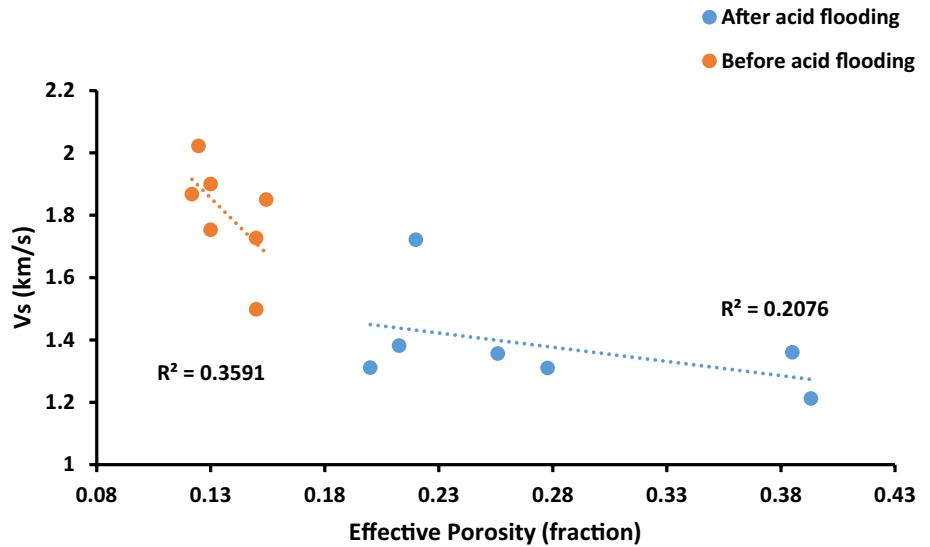
Fig. 9 Relationships between the velocity of shear waves (V_s) and effective porosity before and after acid treatment

surrounding region, reducing reservoir output. As a result, the acidizing process is used to minimize the damage and restore the reservoir's productivity by enabling the hydrocarbons to migrate easily (Ghommem et al. 2015). High-permeability flow pathways are created, and the damage can be removed to increase the well's performance. However, during acidizing operations, acid dissolution of rock minerals can modify the rock's structure, the mineralogy, and the mechanical properties of the artificially fractured rocks (Liu and Mostaghimi 2017).

Therefore, the effects of acid treatment on Young's modulus (E) of the seven rock samples studied are shown in Fig. 10. The Young's modulus (E) values before acid flooding are in the range (1.37 E + 10 – 2.77 E + 10), while after acidizing, the E values are between (8.62 E + 09 – 2.04

E + 10). This implies that the pre-acid treatment values of E showed a general reduction compared to the values after acidizing. As a measure of rock stiffness, materials with high resistance to being compressed (or extended) due to applied stress display larger values of E, while softer, less stiff rocks have lower E values. Thus, the results are indicative of the rocks' weakening post-acid flooding. Since this outcome is for the rock mass, that is, the whole core sample and not only the fractured surface, it implies that a wormhole is created, which causes an increase in void space in the rock and consequently lower seismic velocities; thus, Young's modulus reduces.

The Poisson's ratio (PR) values of the pre- and post-acid-treated rock samples are compared, and the results are shown in Fig. 11. Specifically, the findings revealed that the PR

Fig. 10 Young's modulus (E) values pre- and post-acid treatment of the rock samples
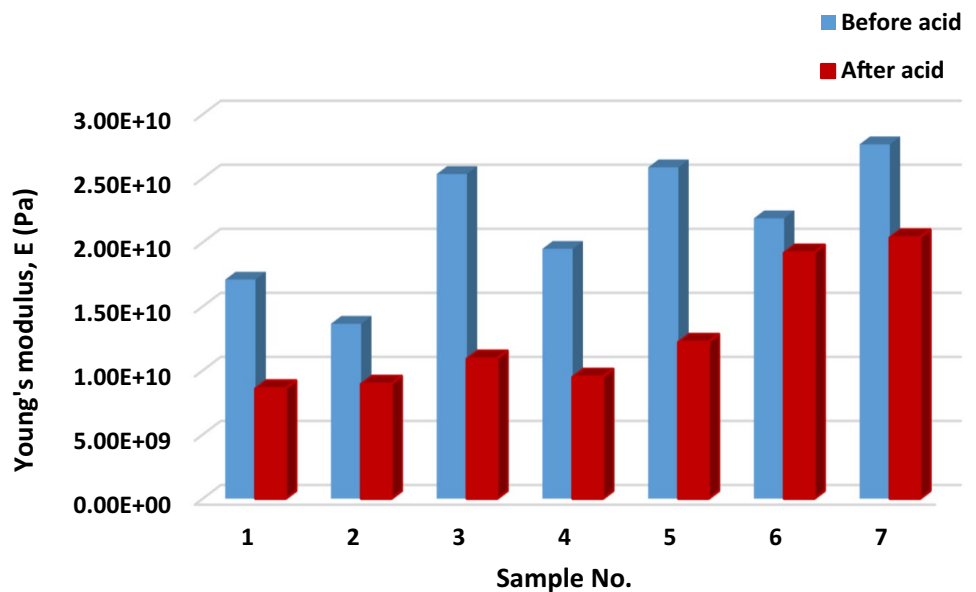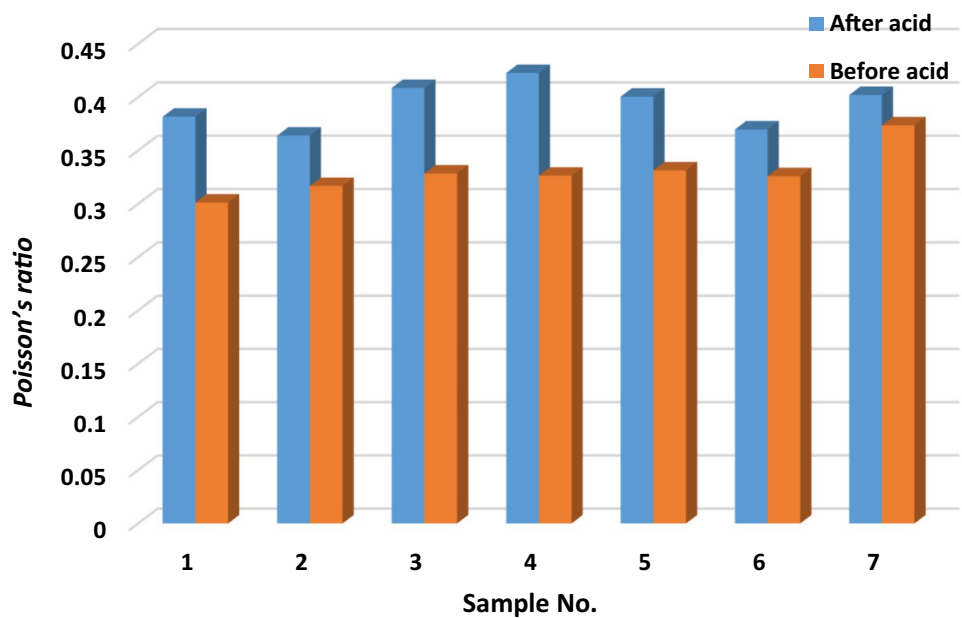
Fig. 11 Poisson's ratio (PR) values pre- and post-acid treatment of the rock samples
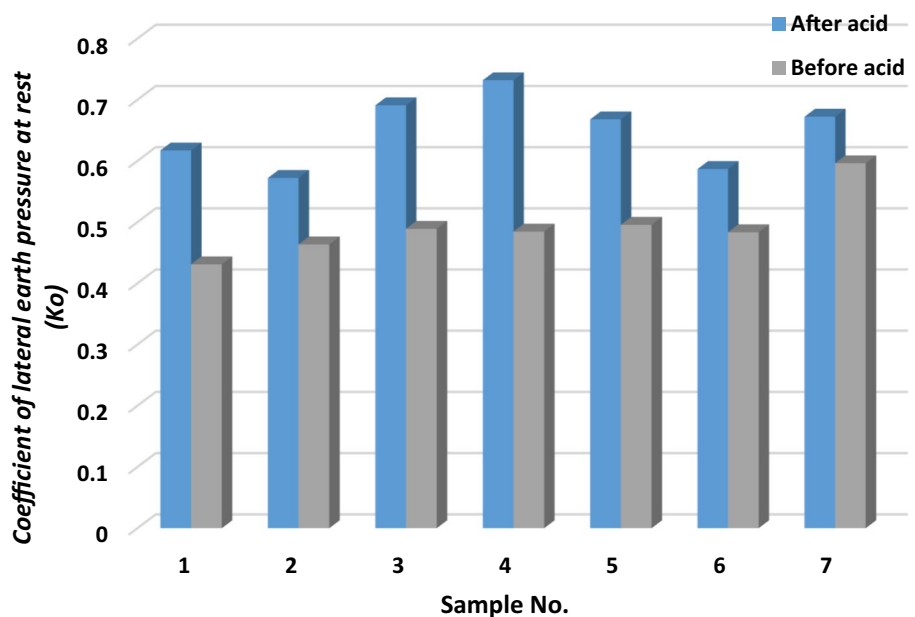

values of the rock samples before acid flooding varied from 0.3 to 0.37, which corresponded to moderately competent rocks. On the other hand, the PR values of the acid-treated rock samples were in the range of 0.36–0.42. Rocks with larger values suggest fracture or wormhole channel, with less rigidity and incompressibility, whereas rocks with lower values indicate moderately intact rocks.

In geotechnical engineering, the coefficient of lateral earth pressure at rest (K_o) is crucial since it influences the strength and consolidation of rocks, as well as the design of engineered structures such as optimal wellbore direction to prevent wellbore instability issues. The knowledge of K_o can be used to optimize stimulation jobs to avoid

sanding after acidizing. From the K_o values obtained, a similar pattern is noted: it decreases for densely consolidated sediments and rises in loosely consolidated strata. Rock samples pre- and post-acid treatment were examined for changes in the values of the coefficient of lateral earth pressure at rest, as illustrated in Fig. 12. A range of 0.43 to 0.59 was found for the K_o values of the rock samples before acid flooding, corresponding to rocks that were moderately consolidated before flooding. The K_o values for the acid-treated plug samples ranged from 0.57 to 0.73. Fractures or wormhole channels are indicated by rocks with higher values, while rocks with lower values exhibit moderately confined pores.

Fig. 12 Values of the coefficient of lateral earth pressure at rest (K_o) pre- and post-acid treatment of the rock samples

Material index (IM) values before and after acid treatment are shown in Fig. 13. In this regard, the parameter's values for the rock samples pre-acid treatment range between -0.2 to -0.49, indicating the hardness of the rocks. On the other hand, the values of this parameter range from -0.45 to -0.63 for the acid-treated rock samples, indicating rock weakening as a result of rock mineral dissolution during the acid reaction. A summary of the mechanical parameters of sample 1 and sample 5 before and after acid treatment is provided in Table 5.

Computed tomography (CT)

In addition to the petrophysical and acoustic measurements, CT scanning was employed to visualize the results of the acid core flooding. Nondestructive 3D imaging was conducted using computed tomography. When X-rays travel through a substance, they are attenuated, and the corresponding material image is formed (Tembely et al. 2021). CT scan has been employed to monitor fracture openings (Martyushev and Yurikov 2021). In this study, acid core-flooding tests were carried out at various injection rates on different rock samples, causing the wormholes to differ in structure from one rock sample to the other and even within the same rock type. The size and nature of the wormhole may be responsible for the change in mechanical and physical characteristics of the rock (Artyushkova et al. 2021; Martyushev et al. 2019; Mustafa et al. 2022; Song et al. 2021; Zhang et al. 2020a). Micro-CT images of two of the acidized rock samples were reconstructed using the 3D Slicer software. A medical CT scanner was used to scan the chosen plug samples before and after acid treatment. Contrast and noise reduction were prioritized while scanning. Figures 14, 15 and 16 show the CT scan of plug sample No. 1 after acid treatment with a flow rate injection of 6.67 cc/min (Figs. 14b and 16a), where the wormhole channel was created as a result of convection, thus forming a wormhole, and plug sample number No. 5 after acid treatment with flow rate injection of 0.667 cc/min (Figs. 15b and 16b), where the acid reaction is the dominant mechanism, thus creating a conical-shaped wormhole (Fredd and Fogler 1999).

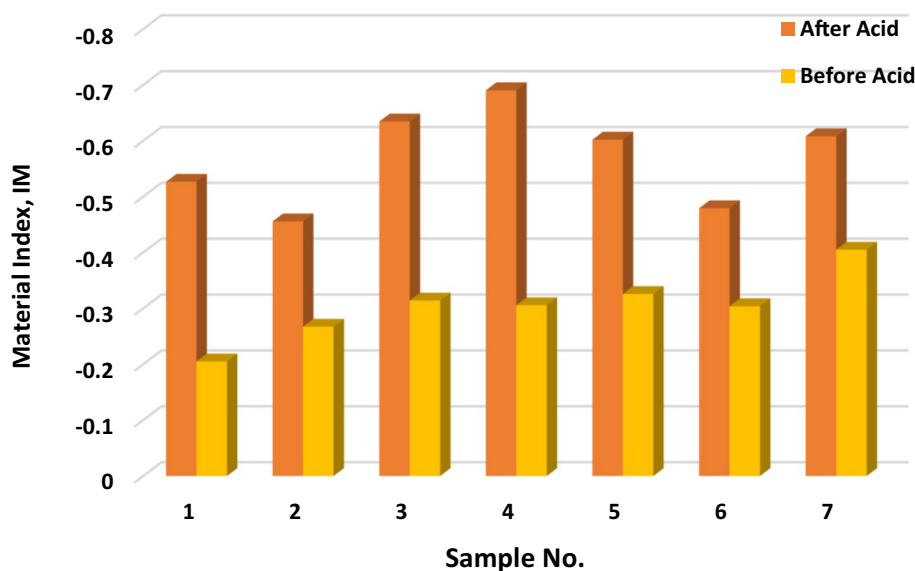Fig. 13 Material index (IM) values pre- and post-acid treatment of the rock samples

Table 5 A summary of the mechanical parameters of sample 1 and sample 5 before and after acid treatment

Sample no	Parameter	Before acid treatment	After acid treatment
1	Young's modulus	1.71E + 10 (Pa)	8.62 + 09 (Pa)
	Poisson's ratio	0.301	0.382
	Coefficient of lateral earth pressure at rest	0.431	0.617
	Material index	− 0.205	− 0.527
5	Young's modulus	2.59 E + 10 (Pa)	1.22 E + 10 (Pa)
	Poisson's ratio	0.331	0.400
	Coefficient of lateral earth pressure at rest	0.496	0.668
	Material index	− 0.326	− 0.602

Fig. 14 CT scan for sample 1: **a** before acidizing and **b** after acidizing with an injection flow rate of 0.667 cc/min
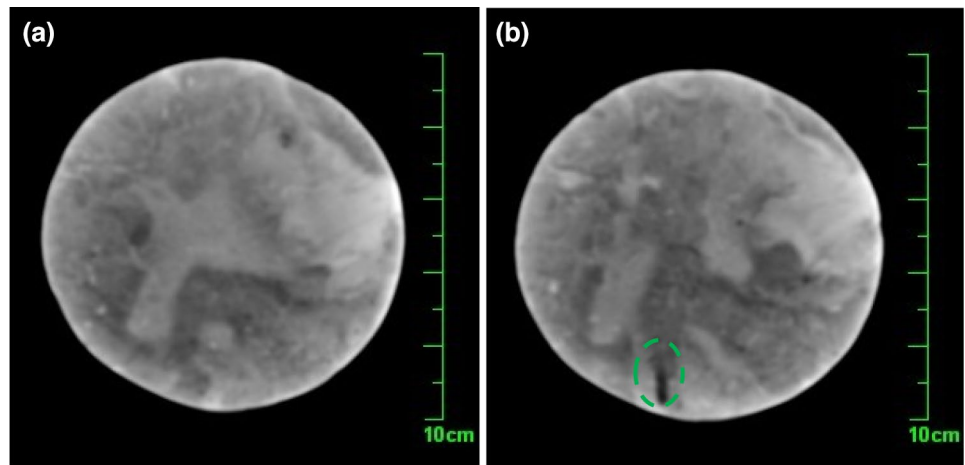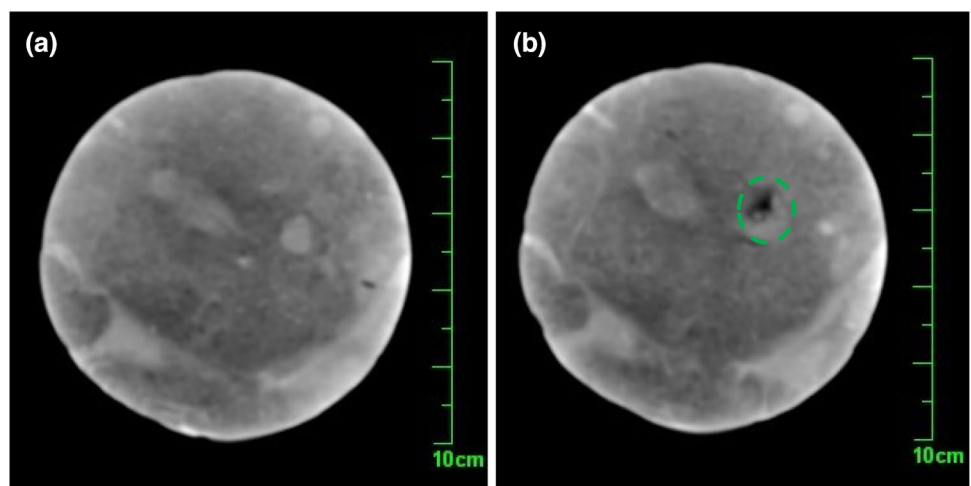

Fig. 15 CT scan for sample 5: **a** before acidizing and **b** after acidizing with an injection flow rate of 6.67 cc/min

Recommendation

In acid flooding, rock weakening does not necessarily mean deterioration/sand production/instability; instead, it depends on other factors. For instance, it could be due to acid-induced fracture/wormhole, which corresponds to porosity enhancement that resulted in lower acoustic readings and thus manifested as reduced rock strength. Accordingly, the following recommendations are drawn:

- We suggest that independent investigations of the bulk rock and fractured surface strength be conducted to be able to make a clear distinction between these occurrences.
- Furthermore, the experimental results presented in this study for the MI4 formation of the Mishrif reservoir demonstrated that despite the observed rock's mechanical properties alterations, which show wormhole propagation, effective wormholes/flow paths were created for hydrocarbon flow from the reservoir into the wellbore.

The results presented implied a successful acid treatment of the Ahdeb oilfield despite the development problems of the Ahdeb oilfield reported (i.e., the high injection pressures that makes acid injection difficult in this reservoir formation and the numerous acidizing job failures) during the stimulation operation of this reservoir formation.

- Formation permeability greatly governs the choice of reservoir acid stimulation technique to be employed, that is, either acid fracture or matrix acidizing. Generally, acid fracturing yield better results in low permeable hard rocks. On the other hand, matrix acidizing is more effective in soft, high permeability formations (Schwalbert et al. 2020). Based on the core and well logs analysis for all of Mishrif's units, permeability values vary from 0.1 mD to 57 mD (see Fig. 2). This shows a broad range of permeability variations; thus, this petrophysical property should be prioritized when planning stimulation operations for the Ahdeb oilfield, particularly in the development of the Mishrif reservoir.
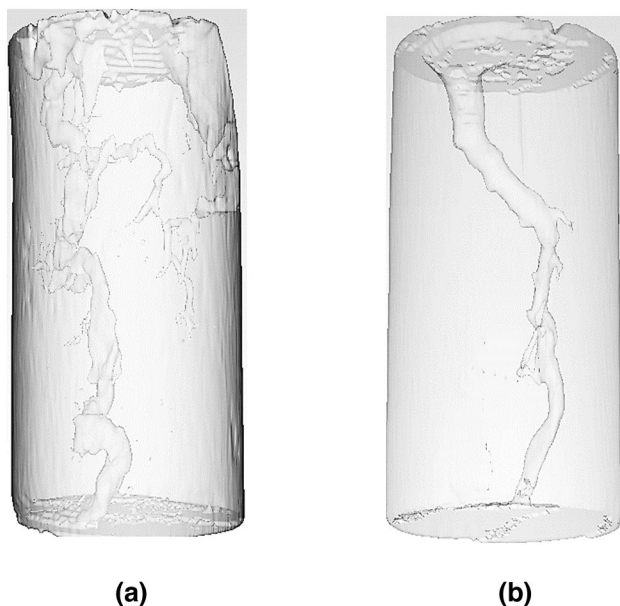
(a)　　　　　　　　　**(b)**

Fig. 16 a Sample 1 after acid treatment with flow rate injection of 6.67 cc/min (wormhole). **b** Sample 5 after acid treatment with flow rate injection of 0.667 cc/min (conical shape)

- Therefore, the high injection pressures reportedly encountered are likely due to injections into zones with very low permeability, such as 0.1 mD zones, thus resulting in the injection difficulties. Moreover, the acidizing jobs failures could also be as a result of wrong choice of acid treatment technique, and it is thus recommended that acid fracturing should be applied for low permeability and hard rock zones, while matrix acidizing should be considered for zones with high permeability in the Mishrif reservoir. Therefore, stimulation design optimization is recommended to reduce these failures as well as injectivity issues.

Summary and conclusions

Significant challenges are encountered during acid stimulation operations in the Mishrif reservoir of the Ahdeb oil field, including high injection pressures, and several acid treatment failures are recorded. The significant failure rate of oil well stimulation in this deposit necessitates more research. Therefore, we presented experimental investigations of the effect of acidizing on the geomechanical properties of the Mi4 formation of the Mishrif reservoir. Several acid-flooding experiments were performed on different rock samples to study the influence of mineralogy and confirm the consistency of the outcomes. The porosity, permeability, acoustic velocities, rock strength, and dynamic elastic

parameters were computed before and after the acidizing treatment. The propagation of an acid-induced wormhole and its effect on the rock strength was analyzed and compared to that of intact rocks. Thus, the following conclusions are drawn:

- We found that the acid treatment resulted in a considerable increase in porosity for all the rock samples.
- A positive relationship between PVBT and the relative increase in porosity for all rock plugs was established. Thus, we concluded that an increase in PVBT will likely results in an increase in porosity and a consequent decrease in the values of the acoustic properties of the rock.
- The acid efficiency curve yielded the lowest pore volume injected at breakthrough of 3.7 PV at 2.16 cc/min; thus, the optimum injection rate that results in the most optimal wormhole and the least quantity of acid being used for this reservoir is 2.16 cc/min.
- Furthermore, the results also demonstrated that the mechanical properties exhibit rock weakening post-acid treatment. The mechanical properties (i.e., elastic modulus, Poisson's ratio, material index, and the coefficient of lateral earth pressure at rest) showed that the rock weakened after acidizing, and this finding is in line with the work of other researchers (Lai et al. 2021; Mustafa et al. 2022; Zhang et al. 2020a).
- Young's modulus for the seven rock samples investigated exhibited a reduction of 26–37%. Conversely, the Poisson's ratio, the coefficient of lateral earth pressure at rest, and the material index increases by 13–20%, 23–32%, and 28–125%, respectively.
- The CT scan visually confirmed that the acid treatment effectively creates a pathway for oil flow from the reservoir to the wellbore.
- It further showed that at low acid flowrate (0.67 cc/min), face dissolution occurred, and a substantial amount of acid was consumed before the wormhole could breakthrough at this rate, thus resulting in shorter, conical-shaped wormholes. At high acid injection rate (6.67 cc/min), a longer and wider wormhole was generated.

Appendix

Comprehensive geological properties of the Mishrif reservoir are provided in Fig. 17. The geology and mineralogy of Mishrif reservoir's well ADM12, Cenomanian Mi_4 formation is shown. Photomicrographs for the two cored sections of the Mishrif reservoir's well ADM12. (a) For samples 1–4: a texture with burrow texture, internal ring is
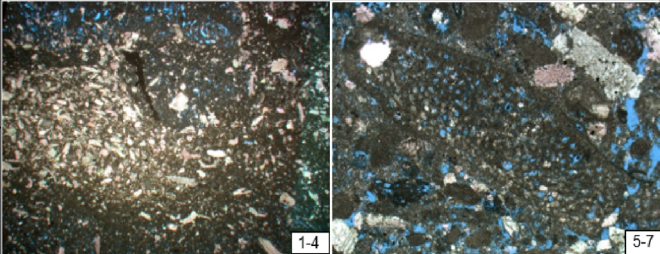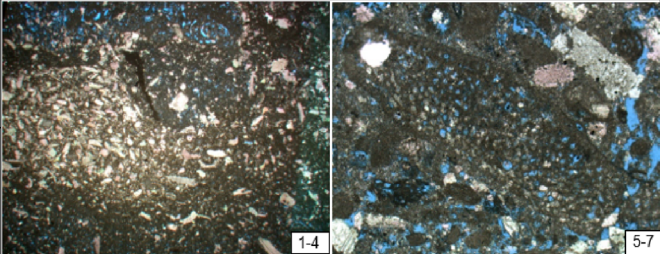
Sample No.	Sampling Formation	Well Interval (m)	Rock Name (Texture、componet or structure)	Calcite	Dolomite	Clay	Fluorite	Pyrite	Terrigenous clast	Foraminifer	Orbitolina	Echinoderm	Brachiopoda	Gastropoda	Pelecypoda	Beehive worm	Bioclast	Bryozoon	Gobigerina	Green algae	Red Algae	Algae nodule	Algae pellet	Oolite	Sand grain	Total	Matrix-supported	Micrite	Sparry	Quantity	Filling degree	Total thin section porosity
1-4	Cenomanian Mi₄	2745.68 ~ 2745.71	Echinoderm green algae micrite limestone	98		1	0.5	0.5		3		10	2	1	3	2	2		5	20						48	52					22.0
5-7		2760.10 ~ 2760.20	Micrite orbitolina sand grain limestone	98		1.5		0.5	1	1	25	5	2	3					1	5					35	77		23		1	30	22.5

	Description
1-4	Very complecate texture with biological burrow texture, innternal ring is composed of echinoderm and core is composed of gastropoda, green algae. Overall texture is echinoderm, green algae micrite texture and large gobigerina and beehive worm in amount.
5-7	Large amount of grain and concentrated in species. Is predominated by orbitolina debrisbystrong solution, also named as orbitolina sand grain, visible dividual orbitolina is stored in good shape. Another is echinoderm with large amount of sand grain with strong solution and dense gathering.

Fig. 17 Geology and mineralogy of Mishrif reservoir's well ADM12, Cenomanian Mi₄ formation

composed of echinoderm. Overall texture is echinoderm, green algae micrite texture, large globigerina, and beehive worm; (b) for sample 5–7: Limestone composed mainly of orbitolina debris, also termed orbitolina sand grain, visible dividual orbitolina and echinoderm with large amount of sand grain with and dense gathering. Table 6. shows the petrophysical and fluids properties of the Mishrif reservoir's Mi₄ formation. The porosity and the effective permeability are 22.2% and $10.32 \times 10^{-3} \mu m^2$, respectively. The residual oil and connate water saturations are 31.23% and 35.09%, respectively.

Table 6 Formation and fluids properties

Parameter	Value/name
Oil field/well	AD—12
Formation	Mi₄
Depth, m	2740.1–2765.9
Sample	1–7
Length, cm	4.571
Porosity, %	22.2
Residual oil saturation, %	31.23
Temperature, ℃	81
Saturated water salinity, mg/L	209,154.30
Bound water saturation, %	35.09
Diameter, cm	25,264.571
Gas permeability,$10^{-3} \mu m^2$	12.7
Water viscosity, mPa.s	0.45
Oil viscosity, mPa.s	1.76
Effective permeability of oil,$10^{-3} \mu m^2$	10.32

Declarations

References

Abd El-Rahman MM, Setto I, El-Werr A (1992) Inferring mechanical properties of the foundation material at the 2nd industrial zone, Sadat city, from geophysical measurements. Egyp Geophys Soc 206:228

Al-Arji H, Al-Azman A, Le-Hussain F, Regenauer-Lieb K (2021) Acid stimulation in carbonates: a laboratory test of a wormhole model based on Damköhler and Péclet numbers. J Petrol Sci Eng 203(February):108593. https://doi.org/10.1016/j.petrol.2021.108593

Al-Awsi MD, Khorshid SZ (2021) Geophysical and geotechnical evaluation of tanjero sandstone layers at dokan area using ultrasonic wave method. Iraqi J Sci 62(7):2262–2271. https://doi.org/10.24996/ijs.2021.62.7.15

Aljawad MS, Schwalbert MP, Zhu D, Hill AD (2020) Improving acid fracture design in dolomite formations utilizing a fully integrated acid fracture model. J Petrol Sci Eng 184:106481. https://doi.org/10.1016/J.PETROL.2019.106481

Al-Yaseri A, Abbasi GR, Yekeen N, Al-Shajalee F, Giwelli A, Xie Q (2022) Effects of cleaning process using toluene and acetone on water-wet-quartz/CO2 and oil-wet-quartz/CO2 wettability. J Petrol Sci Eng 208:109555. https://doi.org/10.1016/J.PETROL.2021.109555

Artyushkova O, Kadyrov R, Fazliakhmetov A (2021) On the possibility of introducing X-ray computed microtomography into the practice of biostratigraphic research. Dspace.Kpfu.Ru. https://dspace.kpfu.ru/xmlui/handle/net/169464

Barri A, Mahmoud M, Elkatatny S (2016) Evaluation of rock mechanical properties alteration during matrix stimulation with chelating agents. J Energy Resour Technol Trans ASME 138(3). https://doi.org/10.1115/1.4032546/373272

Bazin B, Charbonnel P, Onaisi A (1999) Strategy optimization for matrix treatments of horizontal drains in carbonate reservoirs, use of self-gelling acid diverter. All Days. https://doi.org/10.2118/54720-MS

Beckham RE, Shuchart CE, Buechler SR (2015) Impact of acid jetting on carbonate stimulation. https://doi.org/10.2523/IPTC-18360-MS

Dobrin MB (1976) Introduction to geophysical prospecting. McGraw Hill. Int. co (ed.); Internatio

Domenico SN (1984) Rock lithology and porosity determination from shear and compressional wave velocity. Geophysics 49(8):1188–1195. https://doi.org/10.1190/1.1441748

Dong K (2018) A new wormhole propagation model at optimal conditions for carbonate acidizing. J Petrol Sci Eng 171:1309–1317. https://doi.org/10.1016/J.PETROL.2018.08.055

Fjær E, Rune Martin H, Per H, Arne Marius R, Risnes R (2008) Petroleum related rock mechanics

Fredd CN, Fogler HS (1999) Optimum conditions for wormhole formation in carbonate porous media: influence of transport and reaction. SPE J 4(03):196–205. https://doi.org/10.2118/56995-PA

Furui K, Zhu D, Hill AD (2008) A new skin-factor model for perforated horizontal wells. SPE Drill Complet 23(03):205–215. https://doi.org/10.2118/77363-PA

Ghommem M, Zhao W, Dyer S, Qiu X, Brady D (2015) Carbonate acidizing: modeling, analysis, and characterization of wormhole formation and propagation. J Petrol Sci Eng 131:18–33. https://doi.org/10.1016/j.petrol.2015.04.021

Gomaa AM, Nino-Penaloza A, Cutler J, Chaudhary S (2018) Insights of wormhole propagation during carbonate acidizing: a comparison between constant injection pressure versus constant volumetric rate. J Solar Energy Eng Trans ASME 140(10). https://doi.org/10.1115/1.4039443

Gou B, Zhan L, Guo J, Zhang R, Zhou C, Wu L, Ye J, Zeng J (2021) Effect of different types of stimulation fluids on fracture propagation behavior in naturally fractured carbonate rock through CT scan. J Petrol Sci Eng 201(January):108529. https://doi.org/10.1016/j.petrol.2021.108529

Guo J, Liu H, Zhu Y, Liu Y (2014) Effects of acid-rock reaction heat on fluid temperature profile in fracture during acid fracturing in carbonate reservoirs. J Petrol Sci Eng 122:31–37. https://doi.org/10.1016/j.petrol.2014.08.016

Hassan AM, Al-Hashim HS (2017) Evaluation of carbonate rocks integrity after sequential flooding of chelating agent solutions. SPE middle east oil and gas show and conference, MEOS, proceedings, 2017-March, pp 682–696. https://doi.org/10.2118/183760-ms

Isah A, Adebayo AR, Mahmoud M, Babalola LO, El-Husseiny A (2021a) Drainage mechanisms in gas reservoirs with bimodal pores—a core and pore scale study. J Natural Gas Sci Eng 86:103652. https://doi.org/10.1016/J.JNGSE.2020.103652

Isah A, Hiba M, Al-Azani K, Aljawad MS, Mahmoud M (2021b) A comprehensive review of proppant transport in fractured reservoirs: experimental, numerical, and field aspects. J Natural Gas Sci Eng 88:103832. https://doi.org/10.1016/J.JNGSE.2021.103832

Ituen E, Akaranta O, James A (2017) Electrochemical and anticorrosion properties of 5-hydroxytryptophan on mild steel in a simulated well-acidizing fluid. J Taibah Univ Sci 11(5):788–800. https://doi.org/10.1016/j.jtusci.2017.01.005

Jermy CA, Bell FG (1998) Durability of some dolerites from South Africa. Proc 8th Int Cong IAEG 2869–2875

Kiani S, Jafari S, Apourvari SN, Mehrjoo H (2021) Simulation study of wormhole formation and propagation during matrix acidizing of carbonate reservoirs using a novel in-situ generated hydrochloric acid. Adv Geo-Energy Res 5(1):64–74. https://doi.org/10.46690/ager.2021.01.07

Lai J, Guo J, Ma Y, Zhou H, Wang S, Liu Y (2021) Effect of acid–rock reaction on the microstructure and mechanical property of tight limestone. Rock Mech Rock Eng 0123456789. https://doi.org/10.1007/s00603-021-02650-5

Li H, Shi Y (2021) Triaxial experimental investigation into the characteristics of acid-etched fractures and acid fracturing. J Petrol Sci Eng 202:108431. https://doi.org/10.1016/J.PETROL.2021.108431

Li N, Dai J, Liu P, Luo Z, Zhao L (2015) Experimental study on influencing factors of acid-fracturing effect for carbonate reservoirs. Petroleum 1(2):146–153. https://doi.org/10.1016/j.petlm.2015.06.001

Liu M, Mostaghimi P (2017) Pore-scale simulation of dissolution-induced variations in rock mechanical properties. Int J Heat Mass Transf 111:842–851. https://doi.org/10.1016/J.IJHEATMASSTRANSFER.2017.04.049

Lungwitz B, Fredd C, Brady M, Miller M, Ali S, Hughes K (2007) Diversion and cleanup studies of viscoelastic surfactant-based self-diverting acid. SPE Prod Oper 22(01):121–127. https://doi.org/10.2118/86504-PA

Marques EAG (1998) Geotechnical characterization of weathering profiles in biotite gneiss (kinzigites) from Rio de Janeiro City. Engineering Geology : A Global View from the Pacific Rim = Géologie de l'ingénieur : Une Perspective Globale Du Cercle Du Pacifique

Martyushev DA, Vinogradov J (2021) Development and application of a double action acidic emulsion for improved oil well performance: laboratory tests and field trials. Colloids Surf A 612:125998. https://doi.org/10.1016/J.COLSURFA.2020.125998

Martyushev DA, Yurikov A (2021) Evaluation of opening of fractures in the Logovskoye carbonate reservoir, Perm Krai, Russia. Petrol Res 6(2):137–143. https://doi.org/10.1016/J.PTLRS.2020.11.002

Martyushev DA, Galkin SV, Shelepov VV (2019) The influence of the rock stress state on matrix and fracture permeability under

conditions of various lithofacial zones of the tournaisian-fammenian oil fields in the Upper Kama Region. Mosc Univ Geol Bull 74(6):573–581. https://doi.org/10.3103/S014587521906006061/FIGURES/10

Martyushev DA, Govindarajan SK, Li Y, Yang Y (2022) Experimental study of the influence of the content of calcite and dolomite in the rock on the efficiency of acid treatment. J Petrol Sci Eng 208:109770. https://doi.org/10.1016/J.PETROL.2021.109770

Melendez MG, Pournik M, Zhu D, Hill AD (2007) The effects of acid contact time and the resulting weakening of the rock surfaces on acid-fracture conductivity. SPE Eur Form Damage Conf Proc EFDC 2:700–710. https://doi.org/10.2118/107772-ms

Mustafa A, Alzaki T, Aljawad MS, Solling T, Dvorkin J (2022) Impact of acid wormhole on the mechanical properties of chalk, limestone, and dolomite: experimental and modeling studies. Energy Rep 8:605–616. https://doi.org/10.1016/j.egyr.2021.11.249

Ndonhong V, Belostrino E, Zhu D, Hill AD, Beckham RE, Shuchart CE (2016) The impact of rock properties on acid jetting in carbonate rocks: an experimental study. In: Society of petroleum engineers—SPE Europec featured at 78th EAGE conference and exhibition

Safari A, Rashidi F, Kazemzadeh E, Hassani A (2014) Determining optimum acid injection rate for a carbonate gas reservoir and scaling the result up to the field conditions: a case study. J Nat Gas Sci Eng 20:2–7. https://doi.org/10.1016/J.JNGSE.2014.05.017

Schwalbert MP, Aljawad MS, Hill AD, Zhu D (2020) Decision criterion for acid stimulation method in carbonate reservoirs: matrix acidizing or acid fracturing? In: Proceedings—SPE international symposium on formation damage control, January, 19–21. https://doi.org/10.2118/199236-MS

Shafiq MU, Ben Mahmud HK, Arif M (2018) Mineralogy and pore topology analysis during matrix acidizing of tight sandstone and dolomite formations using chelating agents. J Petrol Sci Eng 167:869–876. https://doi.org/10.1016/J.PETROL.2018.02.057

Shirani M, Mathes M, Härkegard G (2010) Three dimensional characterization of defects using x-ray computed tomography. In: 18th European conference on fracture: fracture of materials and structures from micro to macro scale, pp 1–6

Song R, Wang Y, Sun S, Liu J (2021) Characterization and microfabrication of natural porous rocks: from micro-CT imaging and digital rock modelling to micro-3D-printed rock analogs. J Petrol Sci Eng 205:108827. https://doi.org/10.1016/J.PETROL.2021.108827

Tariq Z, Aljawad MS, Hassan A, Mahmoud M, Al-Ramadhan A (2021) Chelating agents as acid-fracturing fluids: experimental and modeling studies. Energy Fuels 35(3):2602–2618. https://doi.org/10.1021/ACS.ENERGYFUELS.0C04045

Taylor KC, Nasr-El-Din HA (2001) Laboratory evaluation of in-situ gelled acids for carbonate reservoirs. All Days. https://doi.org/10.2118/71694-MS

Tembely M, AlSumaiti AM, Alameri WS (2021) Machine and deep learning for estimating the permeability of complex carbonate rock from X-ray micro-computed tomography. Energy Rep 7:1460–1472. https://doi.org/10.1016/J.EGYR.2021.02.065

Walle LE, Papamichos E (2015) Acidizing of hollow cylinder chalk specimens and its impact on rock strength and wormhole network structure. OnePetro

Xue H, Huang Z, Zhao L, Wang H, Kang B, Liu P, Liu F, Cheng Y, Xin J (2018) Influence of acid-rock reaction heat and heat transmission on wormholing in carbonate rock. J Nat Gas Sci Eng 50:189–204. https://doi.org/10.1016/J.JNGSE.2017.12.008

Yildiz T (2006) Assessment of total skin factor in perforated wells. SPE Reserv Eval Eng 9(01):61–76. https://doi.org/10.2118/82249-PA

Yoo H, Kim Y, Lee W, Lee J (2018) An experimental study on acid-rock reaction kinetics using dolomite in carbonate acidizing. J Petrol Sci Eng 168:478–494. https://doi.org/10.1016/J.PETROL.2018.05.041

Zhang H, Zhong Y, Zhang J, Zhang Y, Kuang J, Yang B (2020b) Experimental research on deterioration of mechanical properties of carbonate rocks under acidified conditions. J Petrol Sci Eng 185:106612. https://doi.org/10.1016/J.PETROL.2019.106612

Zhang H, Zhong Y, Zhang J, Zhang Y, Kuang J, Yang B (2020a) Experimental research on deterioration of mechanical properties of carbonate rocks under acidified conditions. J Petrol Sci Eng 185(May 2019):106612. https://doi.org/10.1016/j.petrol.2019.106612

Zhang R, Hou B, Zhou B, Liu Y, Xiao Y, Zhang K (2020c) Effect of acid fracturing on carbonate formation in southwest China based on experimental investigations. J Nat Gas Sci Eng 73(November 2019):103057. https://doi.org/10.1016/j.jngse.2019.103057

Zhou B, Jin Y, Xiong W, Zhang J, Lai J, Fang Q (2021) Investigation on surface strength of acid fracture from scratch test. J Petrol Sci Eng 206(November 2020):109017. https://doi.org/10.1016/j.petrol.2021.109017

Zhu H, Deng J, Jin X, Hu L (2015) Hydraulic fracture initiation and propagation from wellbore with oriented perforation. Springer. https://doi.org/10.1007/s00603-014-0608-7

Publisher's Note Springer Nature remains neutral with regard to jurisdictional claims in published maps and institutional affiliations.